

Extraction of Maternal and fetal ECG in a non-invasive way from abdominal ECG recordings using modified Progressive FastICA Peel-off

Yao Li#, Xuanyu Luo#, Haowen Zhao, Jiawen Cui, Yangfan She, Dongfang Li, Lai Jiang*, Xu Zhang*

Abstract — The non-invasive abdominal electrocardiogram (AECG) gives a non-invasive way to monitor fetal well-being during pregnancy. Due to the overlap with maternal ECG (MECG) as well as potential noises from other sources, it is challenging to extract weak fetal ECG (FECG) using surface electrodes. Taking advantage of precise source separation capability of the FastICA approach combined with its constrained version specific to FECG, with weak source extraction capability warranted by the peel-off strategy and FECG waveform reconstruction ability ensured by singular value decomposition (SVD) method, a novel framework for FECG extraction from AECG recordings is presented in this paper. Specifically, a periodic constrained FastICA (pcFastICA) was developed to improve the precision of examining and correcting FECG source signals, based on the statistical characteristics of continuous and repetitive ECG emissions. Additionally, a successive judgement algorithm is designed to selected the optimal maternal and fetal ECG. The performance of the proposed method was examined on public datasets, synthetic data and clinical data, with an F1-scores for FECG extraction on ADFECG and NIFECGA dataset of 99.71% and 99.36%, on synthetic data with the highest noise level of 98.77%, on clinical data of 98.09%, which are all superior to other comparative methods. The results indicates that our proposed method has potential and effectiveness to separate weak FECG from multichannel AECG with high precision in high noise condition, which is of vital importance for ensuring the safety of both the fetus and the mother, as well as the advancement of artificial intelligent clinical monitoring.

Index Terms—Multichannel abdominal ECG, fetal ECG, periodic constrained FastICA

I. INTRODUCTION

ANNUALLY, around 2 million stillbirth occur worldwide[7]. The monitoring of fetal electrocardiography (FECG) offers valuable insights into fetal heart rate (FHR), heart rate variation, and other pertinent data[9], enabling obstetricians to assess maternal and fetal health throughout pregnancy[10], which plays a crucial role in reducing perinatal morbidity and mortality associated with a wide range of fetal heart anomalies [11].

To obtain the clinical information on activities of the fetal heart non-invasively, many electronic devices have been applied for fetal cardiac assessment, including cardiocography (CTG) [12], Doppler ultrasound [16], fetal magnetocardiography (FMCG) [18], fetal phonocardiography (PCG) [19] and fetal electrocardiography (FECG)[20]. However, CTG, although widely used [21], is susceptible to signal loss [22]and inaccurate heart rate estimation. Additionally, both CTG and Doppler ultrasound carry inherent safety concerns due to the use of high-frequency ultrasound signals directed towards the fetus[14, 23]. Fetal PCG, while useful, is sensitive to sensor placement[24] and requires extensive data processing to distinguish fetal cardiac signals from background noise[21, 25]. Considering the limitations of existing tools, FECG emerges as a recommended and safe technology for accurately capturing fetal cardiac activity[16, 26], offering precise beat-to-beat FHR acquisition and promising prospects for long-term monitoring.

Although FECG collection is relatively convenient and can non-invasively reflect the fetal heartbeat, it still faces challenges. As FECG signals propagate from the body to the surface, they pass through a series of body tissues, therefore have relatively small amplitudes[27]. Moreover, the AECG signals we collect from the surface of the maternal skins are signals mixed with various sources and noise, include maternal ECG (MECG) signal, fetal peristalsis, electromyographic (EMG) signal, power line interference and motion artifacts, overlapping the FECG in both frequency and time domains [28-31]. Therefore, extracting the R-peak from the mixed signal is a crucial step in using FECG for fetal heart monitoring[17].

In order to make convenient, non-invasive fetal heart monitoring available via surface-collected FECG signals, researchers have explored numerous methods to extract accurate FECG signals from high-noise surface environments[26, 32, 33]. Methods based on adaptive filtering (AF)[1, 2, 34] suppresses the influence of MECG with the help of reference signal recorded on the chest. However, literature[35, 36] shows that the final FECG still contains the MECG signal after the above methods. Template subtraction (TS)[37, 38] methods eliminate MECG components by subtracting MECG template from NIFECG. However, the average MECG template may be distorted by overlapping or false heartbeat detection cycle, and the MECG morphology is

Y. Li, X. Luo, H. Zhao, J. Cui, Y. She, D. Li, X. Zhang are with the School of Microelectronics at University of Science and Technology of China, Hefei, Anhui, China. (xuzhang90@mail.ustc.edu.cn).

also sensitive to many factors including electrode configuration and body posture [33]. The wavelet -based methods[39-41] make use of intrinsic multifaceted property to manipulate R-peak identification. Nevertheless, a suitable wavelet base should be selected before, showing low robustness[19, 21]. Deep learning (DL) methods[5, 15, 16, 42-44] extract nonlinear feature and map FECG and MECG from AECG simultaneously. Although good performances are reported in the DL solution, it is very time-consuming and the result heavily relies on the training data.

Due to the nature of the collected electrophysiological signals being a superposition of different sources, we can also consider using blind source separation (BSS) based methods when extracting FECG signals. Independent component analysis (ICA)[32], principal component analysis (PCA) and non-negative matrix factorization (NMF)[8] have been used to extract FECG signals. Despite traditional BSS methods operated well in some of records, in some cases these methods could not detect a clean FECG sufficiently[45]. By incorporating the reasonable assumption of pseudo-periodicity, the performance of periodic component analysis (π CA)[46] and the dual self-calibration algorithm proposed by Qiao et al.[17] have been significantly improved. Unfortunately, even with the addition assumption of pseudo-periodicity to the basic blind source separation algorithm, it still struggles to perform well in high-noise environments. The basic blind source separation can only achieve preliminary separation of signals, often having remained noise in high-noise environments, thus affecting the accuracy of fetal heart monitoring. Additionally, since the mixed signal includes MECG that also exhibits pseudo-periodicity and has a much larger amplitude than the faint FECG, in practical applications, algorithms like ICA, which based on gradient descent, tend to converge towards the larger MECG, resulting in local convergence, therefore enable to accurately extract the faint FECG. Therefore, these approaches were not satisfactory for high noise condition.

In recent years, Chen et al. [47-52] introduced a novel method known as progressive FastICA peel-off (PFP) within the realm of EMG decomposition. This approach addresses a range of challenges in EMG decomposition by employing an innovative framework. Their approach involves refining more accurate motor unit (MU) spikes from the spikes initially extracted by FastICA, utilizing constrained FastICA. Furthermore, they employ a peel-off strategy to avoid local convergence to larger MU spikes. Inspired by their work, we can learn from their ideas to tackle the challenges we face in extracting weak FECG signals.

In this study, we present a novel FECG progressive FastICA Peel-off framework consists of FastICA, periodic constrained FastICA (pcfICA), SVD and peel-off strategy to achieve high robustness and good-quality FECG detection. The combination of FastICA and pcfICA can correct the obtained MECG and FECG spikes, resulting in more accurate MECG and FECG spikes. By estimating the waveforms of spikes in the corresponding channels using SVD and subtracting them, a peel-off effect is achieved, preventing the algorithm from converging to larger MECG and noise, thereby improving the extraction performance of faint FECG signals. Our method gives path to reliable non-invasive FHR monitoring in clinical practice.

II. RELATED WORKS

A. The PFP method

The implication of PFP is to expend the constituent motor unit spike trains (MUSTs) set from surface EMG progressively. Automatic PFP (APFP)[48], termed as the automatic version of PFP, is described here. The recording multichannel EMG was first preprocessed and divided into data segments according to the force task. Then, the EMG segment was first fed into the BSS model composed of extension and whitening process and FastICA. Through this processing, the signal was separated into a set of source signals and corresponding separation vectors. Due to the severe MUAP overlapping and MU firing synchronization, a self-calibration implementation consist of valley-seeking clustering method[53] and constrained FastICA[52]. The MU spikes from the same motor unit were clustered then used as constraints to converge. Thus, some error spikes in the extracted source signals could be corrected during this approach. To evaluate the reliability of decomposed MUSTs, a series of metrics was applied comprehensively[48, 49]. If the decomposed MUSTs pass the judgement, the MUAP waveform was estimated and peel-off from signal to encourage more MUs emerge in the next iteration. For more details, please refer to [48-51, 54].

B. Data model

It is assumed that AECG signal is the superposition of the MECG, the FECG and the sum of noises recorded at each surface electrode. Based on the assumption that for each source, the waveform and amplitude observed by electrodes placed on different area are different, shift-invariant convolution model was introduced to represent the AECG $X(t)=[x_1(t), x_2(t), \dots, x_m(t)]^T$. The finite ECG spike responses are the potentials caused by ventricles depolarization. The data model is defined as:

$$x_i(t) = \sum_{j=1}^N \sum_{l=0}^{L-1} w_{ij}(l) s_j(t-l) + n_i(t); \quad i=1,2,\dots,M \quad (1)$$

where $w_{ij}(l)$ denotes the j^{th} ECG waveform of one heartbeat on i^{th} channel; t denotes discrete time; L denotes the waveform length; M denotes the recorded channel number; N denotes the ECG number; $s_j(t-l)$ denotes the binary pulse sequence (i.e. either 0 or 1) on channel j at time t ; $n_i(t)$ denotes the additive noise on i^{th} channel.

As suggested in [54, 55], the convolutive mixture as in equation (1) can be represented as a linear instantaneous mixture of extended sources with K delayed by employing convolution to linearization strategy.

III. METHODS

A. Dataset Description and Preprocessing

1) . Public databases

Two public databases were utilized to validate the effectiveness of the proposed method, which are described as follows.

1) ADFECG. ADFECG[56] database has 5 multichannel records, acquired from 5 subjects between 38 and 41 weeks of

gestation. Each record composed four channels abdominal signals taken from pregnant women's abdomen with a sampling rate of 500 Hz and one reference signal taken from fetal scalp with a sampling rate of 1 kHz. Annotations of fetal R-peak location for datasets were verified by medical experts and provided in the dataset. A bandpass filter(1-100Hz) was applied to the signals during acquisition with filtering of the power-line interference.

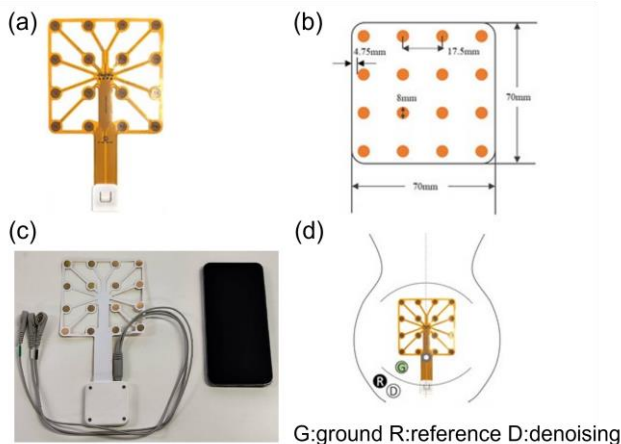
2) NIFECGA. Set-A of the 2013 Physionet/Computing in Cardiology Challenge[57] has 75 AECG recordings with a duration of 60s. Each has four-channel abdominal signals along and one observation obtained from direct fetal scalp ECG with the reference fetal R-peak annotation obtained from the proficient cardiologist. The recording signals are observed at 1 kHz with 16 bits resolution. As suggested in [5, 14, 15, 17, 21], a few records a33, a38, a52, a54, a71, and a74 are discarded from the dataset due to inaccurate fetal R-peak annotations, leaving 69 records for assessment.

Before the actual separation process of AECG signals, several preprocessing steps were undertaken to reduce noise contamination. The impulsive artifacts were removed from each AECG channel, as suggested in [58]. After that, the AECG was filtered with a bandpass filter with the cut-off frequencies of 3 Hz and 100 Hz. Power-line interference as well as its harmonics were removed using a series of notch digital filters. All records in ADFECG database were divided into a series of 60s segments without overlap. These segments were upsampled at 1 KHz for subsequent method.

II) . Clinical data

All clinical data used in this paper were collected at Anhui Provincial Hospital (the first affiliated hospital of University of Science and Technology of China), China. We collected data from the abdominal surface of five healthy pregnant women with gestational ages of 36-40 weeks for subsequent processing and analysis. **All the experiment procedures were approved by the institutional ethics committee of Anhui Provincial Hospital (the first affiliated hospital of University of Science and Technology of China), and the participants' or their conservators' informed consent were given before the experiment.**

Multi-channel AECG signals which contains FECG were collected from the upper abdomen of the participants, using a flexible 4×4 grid electrode array, as shown in



G:ground R:reference D:denoising

Figure 2 (a) 16-channel array electrodes (b) Specific parameters (c) Diagram of electrode placement

(a). Each electrode contact has a diameter of 8mm, and

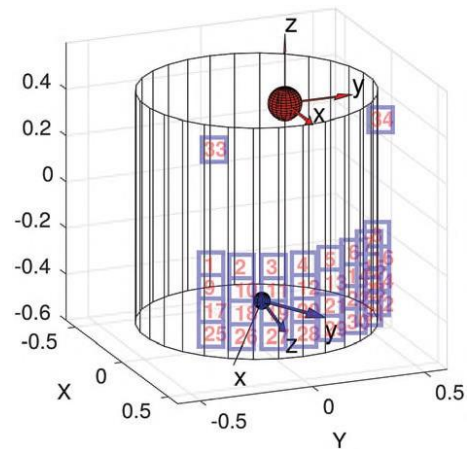


Figure 1 Simulated spatial array for synthetic data

the spacing between electrodes is 17.5mm, as shown in

(b). A wireless multichannel surface electromyogram data recording system (FlexMatrix, Shanghai, China) was used for data recording. It was built with a two-stage amplifier at a total gain of 60 dB, a band-pass filter set at 1-500Hz for each channel and an analog-to-digital converter (ADS1299, Texas Instruments), with a sampling rate of 200Hz, as shown in

(c). During the experiment, we attached the electrodes of the wireless data acquisition device to the pregnant women's abdomen, as shown in

(d) and transmitted the data to a mobile app via Bluetooth for storage and processing.

Several steps were taken to reduce the noise contamination in the pre-processing procedure. The recorded sEMGdi signals were filtered by a Butterworth bandpass filter set at 3-99 Hz to eliminate the potential low-frequency motion artifacts and high-frequency interferences. Then, a set of notch filters were utilized to reduce the effect of power line interference as well as its harmonics.

III) . Synthetic data

The synthetic data used in this study are sourced from the Fetal ECG Synthetic Database (FECGSYNDB), obtains fetal-maternal mixtures by treating each abdominal signal component (e.g. fetal/maternal ECG or noise signals) as an individual source, whose signal is propagated onto the observational points ('electrodes', see Figure 1). Each recording includes the AECG signals along with separate ground-truth maternal ECG (MECG) and fetal ECG (FECG) signals, which consists of 5 minutes of data sampled at 250 Hz. For more details, please refer to[59, 60].

In this study, all 32 channels distributed across the abdominal region, as illustrated in Figure 1, were utilized. Since the ratio between MECG and FECG remains relatively constant in practical cases, five sets of data with signal to noise ratio of the FECG relative to MECG(SNR_{fm}) of -9dB and signal to noise ratio of the MECG over noise (SNR_{mn}) of 6, 3, 0, -3 and -6 dB, therefore achieve a signal to noise ratio of FECG over all noises and interference(SNR_{fn}) of -3,-6,-9,-12,-15 dB were employed to investigate the performance of the methods under different levels of noise.

B. FECCG extraction framework

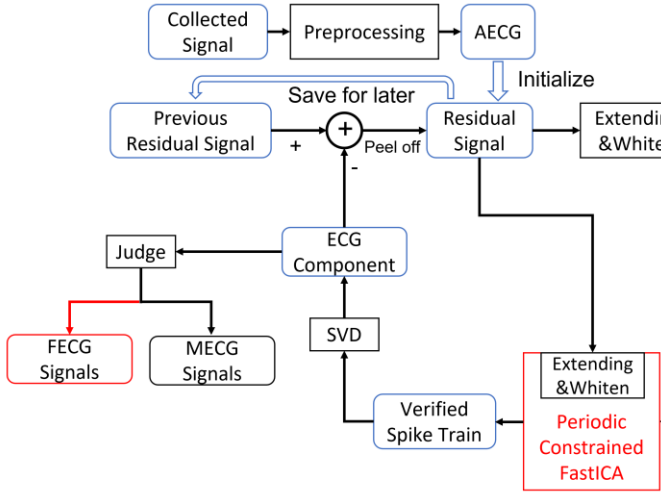


Figure 4 illustrates the flowchart of framework used in this study, which includes preprocessing, periodic constrained FastICA, SVD and peel-off strategy. The collected signals is subjected to high-pass, low-pass and band-stop filtering, finally acquired the preprocessed AECG. The AECG is then feed into source separation module as the initial residual signal. FastICA is used on extended and whitened residual to get preliminary source signals. With the clustering and selection module we are able to get ECG source signals which may be MECG or FECG signals. After we get spike train of ECG signals with QRS detection module, the periodic constrained FastICA is used to get verified spike train. SVD is then used to reconstruct ECG waveforms and then be subtract from residual signals which is peel-off strategy. The reliability judgement module is used to determine whether the output is FECG or MECG. Then the updated residual signal is used for next round of source separation.

I) . Initial Source Separation using FastICA

The data segment was separated into source signals that contain information of maternal or fetal ECG by FastICA. The source signals were extracted by iterative threshold Otsu algorithm[48] and sampling points with amplitude lower than threshold were labeled as no R-peak firing event, as shown in

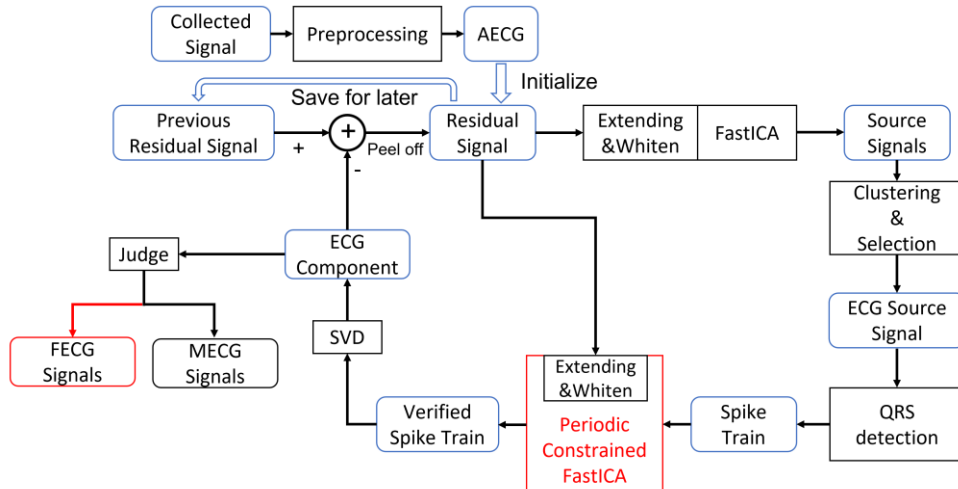


Figure 4 Flowchart of the FECCG extraction framework

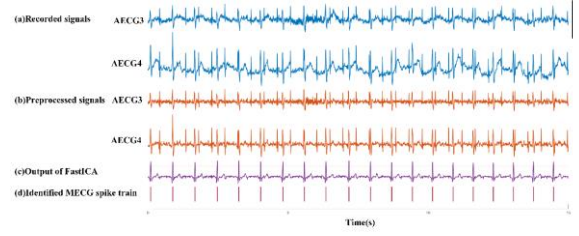


Figure 3. An example of ECG source signal ECG spike identification. The recorded signal is 15s AECG segment from ADFECG database. (a)Recorded AECG on channel 3(AECG3) and channel 4(AECG4). (b)Preprocessed AECG signals on channel 3(AECG3) and channel 4(AECG4). (c)Output source signal of FastICA. (d)Spike train identified from (c).

Figure 3(c) and (d) respectively. Then the initial spike trains was clustered by successor valley seeking approach[53] to distinguish the spikes from the same source signal.

II) . Spike Calibration using periodic constrained FastICA

Although the sources obtained through FastICA have a rough shape, they are only preliminarily separated signals which still contain some noise therefore cannot accurately extract spikes[52]. To prevent errors stemming from potential faults or missing spikes, cfICA was implemented to verify the reliability of FastICA results. In experiments involving FECCG extraction, we noted instances where cfICA underperformed, particularly when noise, such as EMG, interfered with the signal, especially when the FECCG amplitude was lower than that of the noise. Extracting FECCG became challenging for cfICA with only equality constraints when noise competed with FECCG amplitude. Based on the characteristics of the ECG signal, we introduced a periodicity constraint termed periodic constrained FastICA (pcfICA). As a result, pcfICA, combining equality and periodicity constraints, achieved convergence to a reliable spike train.

For equality constraint, the initial spike trains served as an equality constraint[52] to guarantee the convergence toward the component. For periodicity constraint, autocorrelation was used as a loose constraint so that the algorithm tends to converge toward the high periodic component.

Considering constraints mentioned above, the general

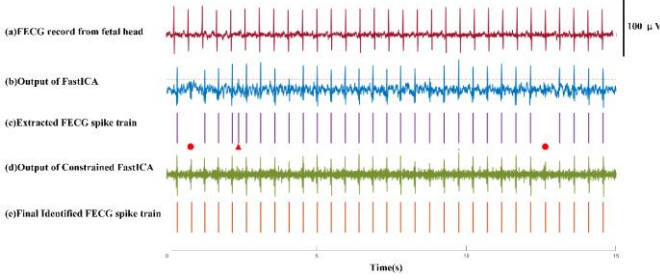


Figure 5. An example of the pcfICA for correcting possible erroneous or missing spike during the decomposition process. (a) FECG recorded from the fetal head. (b)FastICA output corresponding to FECG by applying FastICA on the residual signal. (c) FECG spike train after applying a threshold to (b), with indicating missing spike location denoted as \bullet , error spike location denoted as \blacktriangle . (d) Output of the pcfICA, where those of missing or error spike has been corrected. (e) Final identified FECG spike train to (d) that matches with (a).

problem of pcfICA is given as:

$$\begin{aligned} \max \quad & J_c(w) = [E\{G(w^T x)\} - E\{G(v)\}]^2 \\ \text{st} \quad & g_1(y) = \xi_1 - E\{y^T r\} \leq 0 \\ & g_2(y) = \xi_2 - E\{y^k y\} \leq 0 \\ & H(w) = \|w\|^2 - 1 = 0 \end{aligned} \quad (2)$$

where $J_c(w)$ is the same objective function defined as Eq. 2; $g_1(y)$ is an equality constraint[61] that measures the correlation between the estimated independent component $y = w^T x$ and the reference spike train r ; $g_2(y)$ is the periodicity constraint[46, 62] with respect to the signal y and its delay signal y^k for time lag $k = 0, 1, \dots, N-1$; $\xi_j (j=1, 2)$ denotes the threshold for the lower bound of the constraints. The optimization problem was solved by augmented Lagrangian method[62]. After the cfICA converged, the calibrated spike train was obtained using R-peak detection procedure proposed in [4].

In Figure 5, an example of FECG spike train calibration using the pcfICA is illustrated. Figure 5 (a) shows 15s FECG recorded from the fetal head as gold standard from ADFECG. The output of FastICA by applying FastICA on residual signal that corresponds to FECG is demonstrated in Figure 5 (b). Figure 5 (c) shows initial FECG firing spike train in which it can be seen that some artifact (denoted as \blacktriangle) and missing firing spikes (denoted as \bullet) emerged, which leads to performance degradation. With reference in Figure 5 (b), the output of the cfICA is illustrated in Figure 5 (c). Finally, correct FECG spike train was obtained in Figure 5 (e) that matches with FECG spikes in Figure 5 (a).

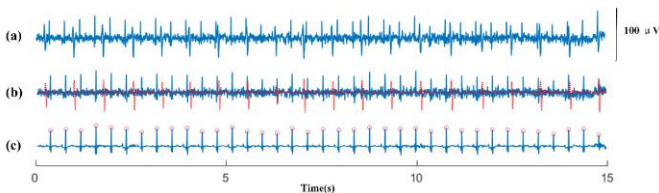


Figure 6. An example of waveform estimation and cancellation by SVD. (a) Recorded AECG on channel 3(AECG3). (b) Estimated waveform (dash red line) estimation by SVD and residual signal after MECG cancellation (blue line). (c) Estimated waveform by SVD using identified R-peak marked by red dot.

III) . Waveform Estimation using SVD

Considering the variable beat to beat interval and periodic ECG waveform, SVD[4] was introduced to estimate the new identified ECG spike train waveform from the current signal, as shown in 错误!未找到引用源。 . The effects and benefits of SVD will be discussed in the Discussion section.

For each channel in signal with q beat period, we utilize the reliable ECG spikes estimation from constrained FastICA to calculate the mean RR interval value p to construct an $p \times q (p > q)$ signal matrix X . And then, X was divided by SVD to obtain the singular value matrix and two orthogonal matrices:

$$X = USV^T \quad (3)$$

where $S = [\text{diag}(\sigma_1, \sigma_2, \dots, \sigma_q), 0]$, $\sigma_1 > \sigma_2 > \dots > \sigma_q$ denotes singular value matrix; $U = [u_1, u_2, \dots, u_q]$, $V = [v_1, v_2, \dots, v_q]$ denotes the left and right singular matrix. X can be indicated by the multiplication of u_i, v_i and σ_i , while σ_i represents the energy distribution of different matrix. Empirically, a subspace of dimension 3 was selected[58].

IV) . Peel-off Strategy for Weak FECG Separation

By using the two-step combination of FastICA and constrained FastICA, we are able to separate the desired sources from the signals. However, considering that FastICA is easily affected by initialization and usually converges to local optimal value, it is difficult for FastICA to find low FECG spikes train[52]. The peel-off strategy was introduced to mitigate the influence of identified ECG spike trains. In each iteration, we first calculate the accurate MECG or FECG spike, and then use SVD to obtain its estimated waveform \hat{X} in each channel. Then the residual signal $X = X - \hat{X}$ can be update, which \hat{X} represents the residual signal from the previous iteration and X represents the estimated waveform of MECG or FECG in this iteration. This approach ensures that each weak EMGdi components are identified, each obtained EMGdi component is unique, and prevents the algorithm from converging locally to larger ECG signals each time.

V) . Peel-off Strategy for Weak FECG Separation

To ensure the separated spike train is true ECG spike train or not, the successive judgement was designed for our clinical PFP method. First, we defined a candidate spike train set φ at the start of procedure. Then, after the convergence of pcfICA, the following criteria was considered: (1) If the R-peak firing rate (denote as Fr) of candidate spike train was lower than 1.11Hz or higher than 3.33Hz, we abandoned the spike train to avoid potential interference. (2) If the correlation (denoted as COR) between two spike trains higher than 0.5, we processed the duplicated spike train by discarding one of them. (3) If the spike train with the index of quality (denoted as IOQ) for the best MECG component identification[4] higher than 6, we added the spike train into φ . (4) The stability coefficient (denoted as SC) which composed of the variation of R-R interval (denoted as cov_{rri}) and the variation of ECG spike amplitude (denoted as cov_{amp}) was defined as follows: $SC = \alpha_1 cov_{rri} + \alpha_2 cov_{amp}$, where α_1, α_2 were set to 100, 1 respectively. If SC was lower than 5, we added the spike train

into φ . For the above criteria, once a validity spike train was added into φ , the residual AECG signals were update by employing peel-off procedure to subtract the waveform of the identified spike train from itself. For further details on the peel-off strategy, please refer to [52]. Next, after employing the clinical PFP until no new satisfied spike train emerged, the spike train with highest IOQ and lowest SC in φ was selected as maternal and fetal ECG spike train respectively. The pseudocode of the clinical PFP is illustrated in Algorithm 1.

Algorithm 1. Framework for fetal ECG extraction

```

1: Initialize residual signal  $\bar{x}$  as AECG. Initialize candidate spike train set  $\varphi = \emptyset$ ,  $Flag=1$ 
2: Extend and whiten  $\bar{x}$  then perform FastICA to extract spike train  $\tilde{v}_1, \tilde{v}_2, \dots, \tilde{v}_n$ 
3: while  $Flag=1$  do
    Flag=0
    for  $i=1; i < N+1; i++$  do
        Apply periodic constrained FastICA on  $\bar{x}$  using  $\tilde{v}_i$  as constraint (termed as  $\tilde{v}_i$ ) of  $\tilde{v}$ .
        if  $Fr(\tilde{v}_i) < 1.11\text{Hz}$  or  $Fr(\tilde{v}_i) > 3.33\text{Hz}$ 
            continue
        end if
        while  $\varphi_j \neq \text{None}$ :
            if  $COR(\tilde{v}_i, \varphi_j) > 0.5$ 
                continue
            end if
            if  $IOQ(\tilde{v}_i) > 6$  or  $SC(\tilde{v}_i) < 5$ 
                 $Flag=1$ 
                add  $\tilde{v}_i$  into  $\varphi_j$ 
                estimate the waveform  $\vartheta$  of  $\tilde{v}_i$ 
                update  $\bar{x} = \bar{x} - \vartheta$  and continue
            end if
        end for
        Extend and whiten  $\bar{x}$  then perform FastICA to extract spike train  $\tilde{v}_1, \tilde{v}_2, \dots, \tilde{v}_n$ 
4: Select maternal and fetal ECG spike train from  $\varphi$ .

```

C. Performance evaluation

Statistical analyses were conducted to evaluate the performance of proposed method and comparison methods of FECG extraction. Following the detection of R-peaks in both reference and extracted FECG signals, positive predictive value (PPV), sensitivity (Sen), accuracy (ACC) and F1 score to assess the performance of different methods which are defined as:

$$\begin{aligned}
 Sen &= \frac{TP}{TP + FN} \times 100\% \\
 PPV &= \frac{TP}{TP + FP} \times 100\% \\
 ACC &= \frac{TP}{TP + FP + FN} \times 100\% \\
 F1 &= \frac{2 \times PPV \times Sen}{PPV + Sen} \times 100\%
 \end{aligned} \tag{4}$$

where TP, TN, FP, and FN denote true positives, true negatives, false positives, and false negatives, respectively. TP denote the number of correctly detected R-peak, FN denote the number of missed R-peak and FP denote the number of incorrect detected R-peak. According to [14, 59, 63], if the extracted ECG spike is within 50 ms from the fetal R-peak annotation, it is counted as a fetal R-peak prediction. We also used FHR root mean square error (RMSE_{FHR}) to assess the degree of difference between the FHR of extracted FECG and the ground truth. RMSE_{FHR} is defined as:

$$RMSE_{FHR} = \sqrt{\frac{\sum_{i=1}^n [FHR_i - FHR_i]^2}{n}} \times 100\% \tag{5}$$

where FHR_i represents the ground truth FHR of FECG in the i th minute of the original signal, FHR_i represents the FHR of the FECG extracted using different methods in the i th minute, and n represents the total sample duration. The smaller the RMSE value, the closer the estimated FHR of the extracted FECG is to the actual FHR, demonstrating the method's greater accuracy.

For the synthetic signals, due to the ground truth FECG waveform is available, we also use SNR to evaluate the level of noise suppression after applying different methods on synthetic data with different noise levels, which is defined as:

$$SNR = 10 \log \frac{\|fECG\|^2}{\|fECG - \hat{fECG}\|^2} \tag{6}$$

For synthetic data, FECG root mean square error (RMSE_{FECG}) is also used to assess the degree of difference between the waveform of extracted FECG and the ground truth. RMSE_{FECG} is defined as:

$$RMSE_{FECG} = \sqrt{\frac{\sum_{i=1}^n [FECG_i - \hat{FECG}_i]^2}{n}} \times 100\% \tag{7}$$

where $FECG_i$ represents the i th point of ground truth FECG waveform, \hat{FECG}_i represents the i th point of estimated FECG waveform, and n represents the total sample number.

For clinical data and synthetic data, four representative comparison methods were selected besides proposed method, which includes FastICA, representing traditional blind source separation methods, LMS, representing adaptive filtering,

Table 1 The determination of modules in the ablation study

Method	equality constraint	periodicity constraint	SVD
cfICA	✓	-	-
pcfICA	✓	✓	-
Proposed method	✓	✓	✓

CycleGAN, representing deep learning, and PFP, a commonly used method in electromyographic decomposition.

In addition, we used ablation experiments on public datasets to determine the necessity of each component in the proposed FECG extraction framework. As shown in 错误!未找到引用源。 , the ablation experiments included two constraint methods and different waveform estimation approaches. Firstly, for each method, FastICA was used to output preliminary separations of MEEG and FECG spike trains. Based on this, we first devised the constrained FastICA (cfICA) method, which employed equality constraints for reliability assessment, while the waveform estimation method remained the least squares method originally used in PFP to estimate the averaged waveform of spike locations. The second method, periodic constrained FastICA (pcfICA), utilized periodicity constraints for reliability assessment, while keeping other parts unchanged. For all methods, the final FECG extraction performance was evaluated.

IV. RESULTS

A. Results of public databases

For public databases, Figure 7 illustrates an example of 15sec raw multi-channel AECG of two channels from ADFECG, estimated MEEG and FECG, real FECG recorded from fetal head, and the estimated FHR results with reference

FHR. In Figure 7 (a), two of the four-channel AECG signals used are represented. MEEG (Figure 7 (b)) and FECG (Figure 7 (c)) were extracted from AECG (Figure 7 (a)) using the proposed method. FECF spike in Figure 7 (c) represents the spike train of the extracted FECG, which obviously corresponds accurately to the reference spike train shown in Figure 7 (d). Figure 7 (e) represents the FHR curve of the extracted FECG and the standard FHR curve. It can be seen that the FHR curve proposed by the proposed method differs from the standard FHR curve by up to 2 BMP in the data segment, which is within the acceptable range.

In Table 2, the quantitative metrics for the proposed method and the comparative methods on ADFECG and NIFECGA databases are listed, showing that the proposed method achieves the highest level of performance, with F1 scores of 99.62% and 99.36%, respectively. Compared to LMS and FastICA, the proposed method demonstrates significant improvements across all metrics. The performance of CycleGAN, PFP, and the proposed method is comparable, but the proposed method exhibits better generalization performance, achieving good extraction results across different datasets. In contrast, the other two methods show slight variations in performance when dealing with different datasets. The $RMSE_{FHR}$ also achieve the best performance among all methods.

Figure 9 presents the results of ablative experiments conducted on the NIFECGA database. It can be observed that implementing equality constraints alone for reliable correction

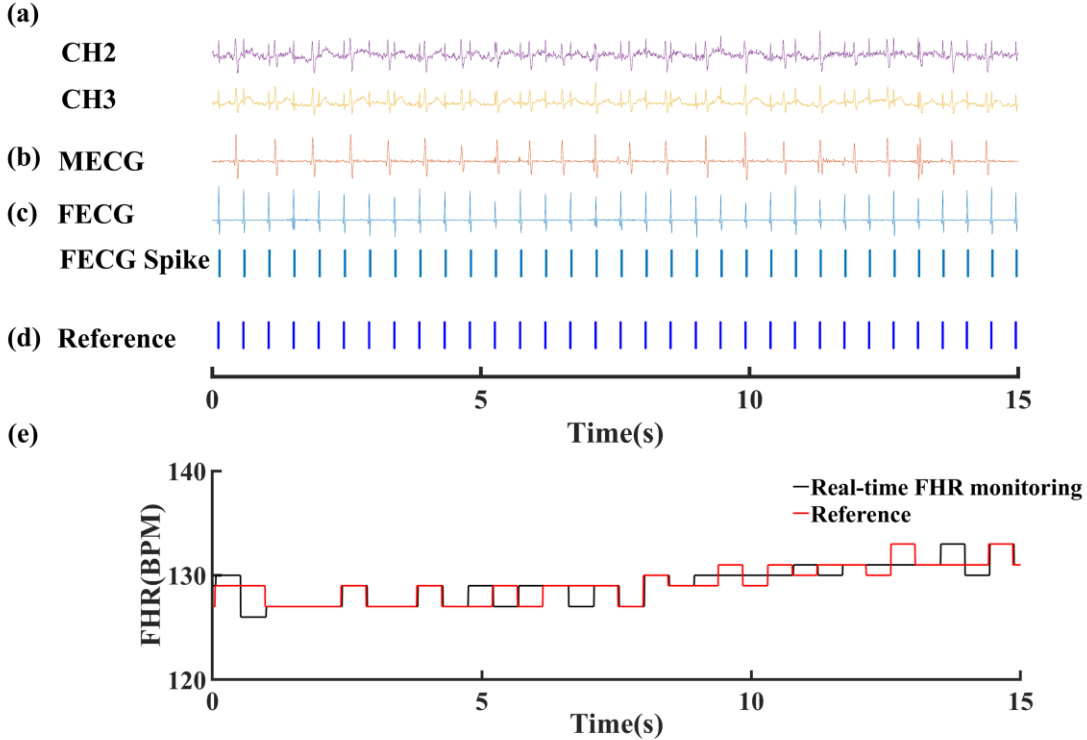


Figure 7. An example of estimated ECG from ADFECG. (a) Recorded AECG on channel 3(AECG1) and channel 4(AECG2). (b) Estimated maternal ECG. (c) Estimated fetal ECG. (d) Spike train extracted from estimated FECG (e) Reference spike train provided by datasets. (e) Real-time FHR monitoring (black line) of FECG compared to reference FHR (red line).

in the cfICA method yields unsatisfactory results, with an F1 score of 96.39%. However, when equality constraints are replaced with periodicity constraints, the performance of the pcfICA method improves, with an F1 score reaching 98.34%. Furthermore, the proposed method achieves the highest performance by utilizing SVD waveform estimation technology, with an accuracy of 98.75%, and all other three metrics exceeding 99%.

in the cfICA method yields unsatisfactory results, with an F1 score of 96.39%. However, when equality constraints are replaced with periodicity constraints, the performance of the pcfICA method improves, with an F1 score reaching 98.34%. Furthermore, the proposed method achieves the highest performance by utilizing SVD waveform estimation technology, with an accuracy of 98.75%, and all other three metrics exceeding 99%.

Table 2 Performance evaluation of different methods on public datasets.

Method	Dataset	SEN (%)	Recordings	PPV (%)	ACC (%)	F1 (%)	RMSE _{FHR} (%)
LMS[3]	NIFECGA	95.8	68	95.0	-	95.4	11.35
FastICA[4]	ADFECG	95.3	5	94.6	-	94.8	9.89
CycleGAN[5]	ADFECG	99.4	5	99.6	-	99.7	4.95
	NIFECGA	96.8	68	97.2	-	97.9	6.04
PFP	ADFECG	97.09	5	98.52	95.69	97.80	8.95
	NIFECGA	99.16	68	98.87	98.11	99.01	8.09
Proposed method	ADFECG	99.75	5	99.50	99.26	99.62	2.48
	NIFECGA	99.46	68	99.26	98.75	99.36	3.03

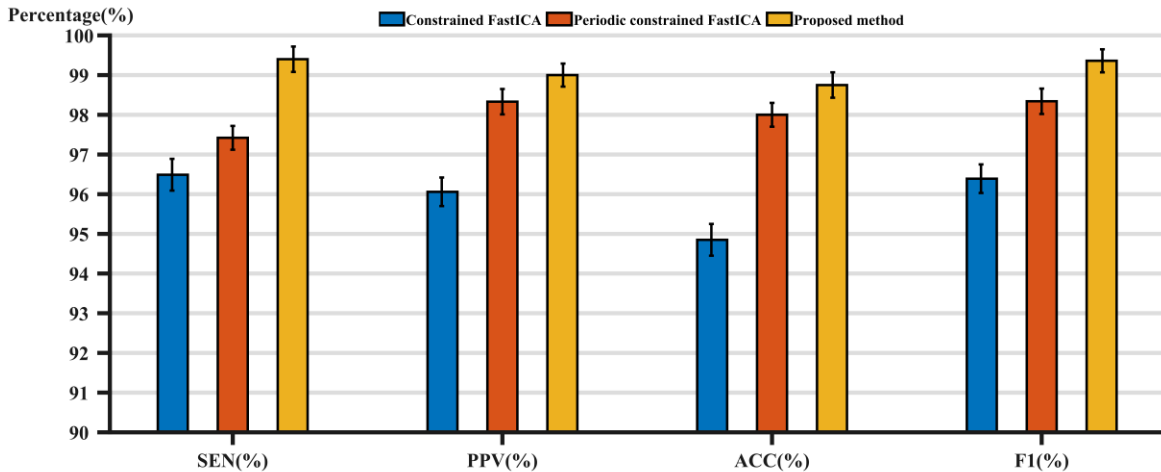


Figure 9. The results of ablative experiments

score of only 96.39%. However, when equality constraints are replaced with periodicity constraints, the performance of the pcfICA method improves, with an F1 score reaching 98.34%. Furthermore, the proposed method achieves the highest performance by utilizing SVD waveform estimation technology, with an accuracy of 98.75%, and all other three metrics exceeding 99%.

B. Results of synthetic data

For synthetic data, we also calculated the FECG extraction performance of the proposed method and the comparative

represents the pure MECG, (b) represents the pure FECG, and (c), (d), (e), (f) I represent the mixed AECG with noise levels of 6, 3, 0, -3, and -6dB, respectively, (c), (d), (e), (f) II represent the corresponding signals extracted MECG, and (c), (d), (e), (f) III represent the corresponding signal extracted FECG. Note that the FECG and MECG contained in each set of noise level signals are specific and are not directly synthesized by (a) and (b), which are just pure signals display and do not represent a specific waveform of a certain group of signals.

Figure 8 shows the quantitative performance metrics of different methods in extracting FECG on synthetic signals,

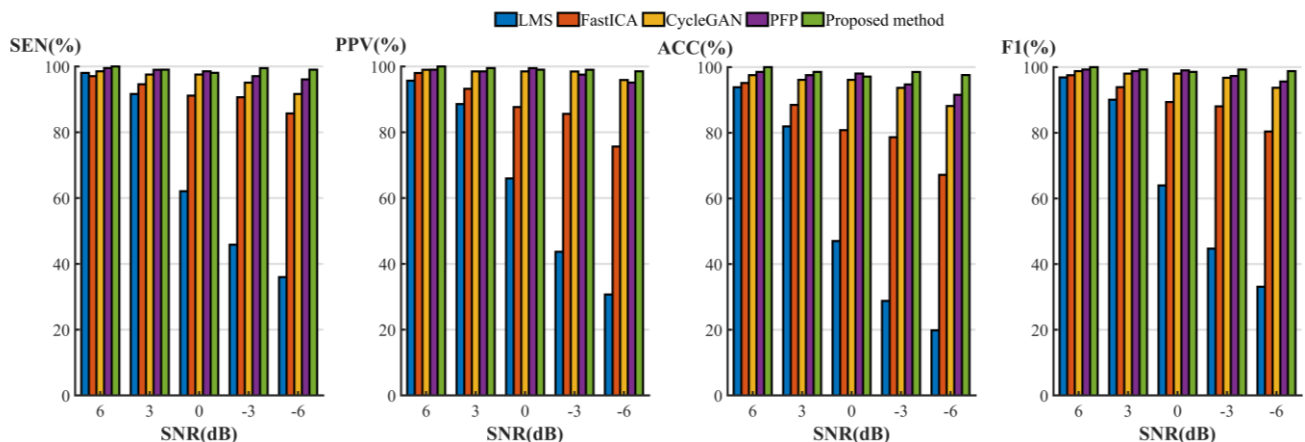


Figure 8. 4 different performance metrics acquired on synthetic data with different MECG to noise SNR of 6,3,0,-3,-6dB by LMS, FastICA, CycleGAN, PFP and proposed method, respectively.

with the pure FECCG of each group of simulated signals as the groundtruth. It can be observed that for data with higher SNR, although the proposed method outperforms other methods, the other methods still achieve acceptable results. However, as the SNR decreases, the performance of morphology-based processing methods such as LMS significantly declines. The performance of FastICA is less affected by the SNR. However, excessive FP and FN resulting from incomplete separation still have a certain impact on its accuracy, especially in high-noise situations where noise is more difficult to remove completely. CycleGAN, as a representative of deep learning methods, still performs well when the FECCG is somewhat overlapped. However, since it utilizes single-channel signals, it still cannot achieve good extraction results when the entire data segment is covered by significant noise and artifacts, thereby affecting the overall extraction performance. PFP achieved results nearly

equivalent to the proposed method, but due to the lack of specific periodic constraints inherent to FECCG, its performance in FECCG extraction was slightly inferior to the proposed method.

Table 3 illustrates the change in SNR after processing synthetic signals with different noise levels using various methods. Compared to other methods, the proposed method shows significant SNR improvement across all noise levels, while other methods exhibit limited SNR enhancement. In some cases, they even have a negative impact on SNR due to poor signal reconstruction performance, leading to inaccurate noise calculation during computation. Although PFP and CycleGAN exhibit good reconstruction performance, their effectiveness in FECCG extraction is slightly inferior to the proposed method, resulting in less SNR enhancement compared to the proposed approach.

Table 3 SNR of extracted FECCG by different methods on synthetic data with different noise levels

SNR _{fm} +SNR _{mn} (dB)	LMS(dB)	FastICA(dB)	CycleGAN(dB)	PFP(dB)	Proposed method(dB)
-9+6	4.39	3.08	13.24	11.90	12.85
-9+3	2.63	2.31	9.84	8.57	10.35
-9+0	-2.91	-2.47	7.90	4.89	6.43
-9+(-3)	-1.43	-1.68	4.38	2.01	7.68
-9+(-6)	-6.56	-2.91	3.29	-3.84	7.32

Table 4 RMSE_{FECCG} of extracted FECCG by different waveform reconstruction methods on different synthetic datasets

SNR _{fm} +SNR _{mn} (dB)	SVD(%)	Least squares(%)
-9+6	10.15	21.85
-9+3	11.03	24.92
-9+0	11.48	25.69
-9+(-3)	10.83	29.59
-9+(-6)	12.39	28.47

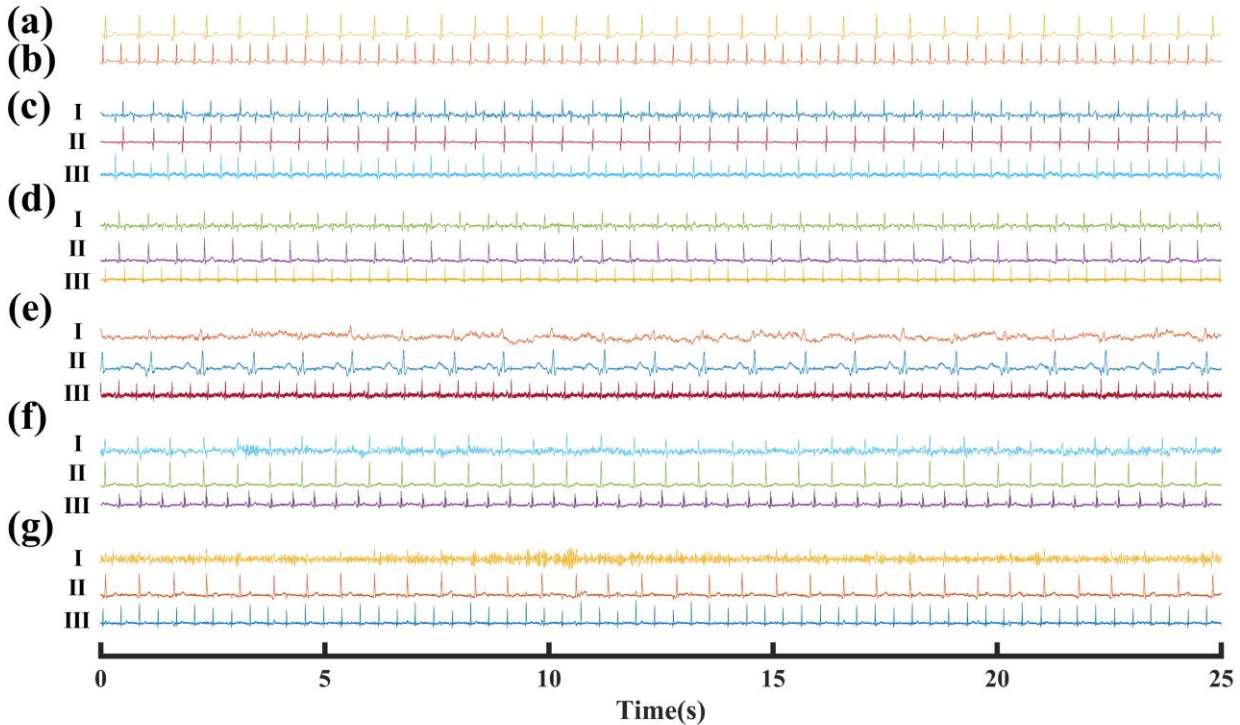


Figure 10 (a) Pure MECCG (b) Pure FECCG (c) I AECG with mnSNR of 6dB II extracted MECCG III extracted FECCG (d) I AECG with mnSNR of 3dB II extracted MECCG III extracted FECCG (e) I AECG with mnSNR of 0dB II extracted MECCG III extracted FECCG (f) I AECG with mnSNR of -3dB II extracted MECCG III extracted FECCG (g) I AECG with mnSNR of -6dB II extracted MECCG III extracted FECCG

We also tested the $RMSE_{FECG}$ between the restored FECG waveform and the pure FECG under different signal-to-noise ratios using different methods, as shown in

Table 4. It can be observed that the performance of SVD in waveform estimation consistently outperforms the estimation methods used in traditional PFP.

C. Results of clinical data

For clinical data, we use manually annotated fetal heart QRS wave positions as ground truth to calculate a series of quantitative metrics. As shown in Figure 11, from (a) the original data without obvious FECG, to (b) the extracted MECG with its spike, to (d) the extracted FECG with its spike, it can be seen that almost all FECG, which were submerged in noise, can be effectively extracted by the proposed methods. For e FECG reference spike train, the spike of extracted FECG obviously corresponds to it. By apply peel-off strategy, that is to subtract (b) from (a) to get residual signal (c), we can avoid local convergence thus extracting weak FECG source signal.

Table 5 shows the number of true positives (TP), false

Table 5 Performance evaluation of different methods on clinical data.

	TP	FP	FN	SEN(%)	PPV(%)	ACC(%)	F1(%)	RMSE(%)
LMS	543	921	1331	28.97	37.09	19.42	32.53	18.04
FastICA	1604	456	270	85.59	77.86	68.84	81.54	12.85
CycleGAN	1744	153	130	93.06	91.93	86.03	92.49	3.90
PFP	1732	235	142	92.42	88.05	82.12	90.18	4.48
Proposed method	1832	42	29	98.44	97.75	96.26	98.09	2.43

positives (FP), and false negatives (FN) of FECG extracted by each method used in five sets of clinical data, along with their quantitative metrics. Due to incomplete removal of noise and MECG, the LMS and FastICA methods have a significant increase in FP, severely affecting the accuracy of fetal heart extraction, despite minor differences in TP. Although CycleGAN exhibits good extraction results in some specific segments, its overall performance is affected by sensitivity to data. The PFP method achieves acceptable performance, but higher FN and FP result in slightly inferior performance compared to the proposed methods.

V. DISCUSSIONS

FECG measurement plays a crucial role in fetal activity monitoring. In clinical FECG measurement, a key challenge is to accurately extract FECG from compound signals. In this study, we present a novel FastICA-based FECG extracting

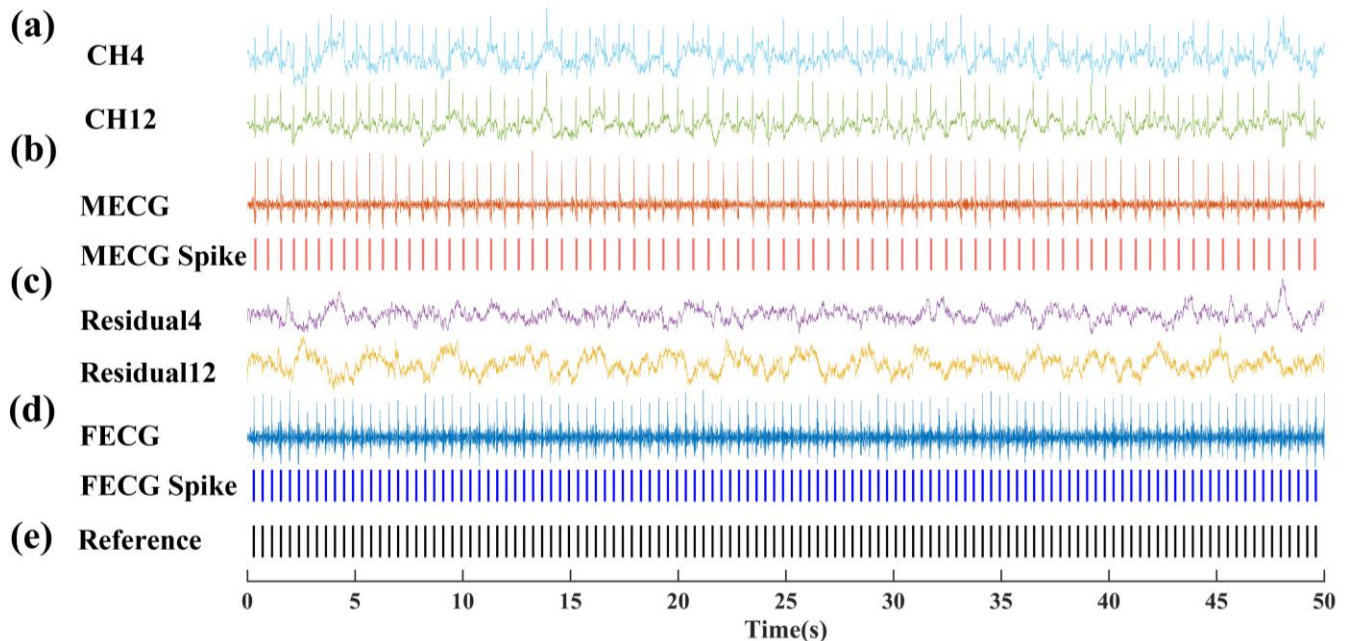


Figure 11. (a) Two channels from the 16-channel clinical data (b) extracted MECG with its spike (c) Two channels from the 16-channel residual signal obtained through MECG peel-off (d) extracted FECG from residual signals (e) Reference signals

framework to extract the weak FECG signals from compound signals acquired from high noise environment. In the proposed framework, the peel-off strategy ensures that the algorithm does not converge locally to large components such as MECG and noise, thus guaranteeing that smaller amplitude FECG can be accurately detected. Moreover, the periodic constrained FastICA algorithm, which incorporates the physiological characteristics of FECG signals, can utilize the prior information obtained from FastICA in the previous step to extract more accurate FECG spike trains and ensure the accuracy of FECG extraction.

Many researchers have tested their methods on public datasets, as shown in Table 6. It can be seen that our method achieves the highest level of performance among these methods, with the highest F1 score. As shown in Figure 7(a), the FECG signals in the public datasets are still clearly visible. This is an ideal scenario in practical applications. For instance, while the methods in [1] and [2] achieve acceptable results on public datasets, their performance decreases on private data. Therefore, although other methods may not perform as well as our proposed method on public datasets, their performance is still acceptable.

We also discuss the performance on synthetic signals for cases with poorer signal quality. In Figure 10, we observe that both our proposed method and other comparative methods achieve high performance when the signal quality is relatively good, in other words, when the MECG to noise SNR is high. In Figure 10 (c), it's evident that FECG in signals with such noise levels are directly observable, reflecting a signal quality level similar to the signal quality of public datasets, as shown in Figure 7 (a). However, as the noise level increases, we observe that FECG signals gradually become submerged in noise and are no longer observable from Figure 10(c) to Figure 10(g). At an MECG to noise SNR of -6dB, even the MECG cannot be

observed. In such cases, the performance of morphology-based LMS significantly deteriorates, from acceptable performance at 6dB to almost no extraction effect at -6dB. FastICA is a commonly used blind source separation method, which separates sources from mixed signals based on multiple channels. When the differences between source signals are large and distinct, FastICA can accurately separate the sources. However, when the noise in the source signals is large, this algorithm can only provide preliminary separation results. In other words, for the desired FECG source signal, some MECG and noise cannot be completely removed, leading to errors in identifying QRS positions and a decrease in accuracy. Previous studies have addressed the issue of preliminary separation by proposing the use of constrained FastICA[52]. By using the sources preliminarily separated as constraints, more accurate spikes can be extracted. In experiments, the results in Figure 8 demonstrate that compared to using only FastICA, the addition of constraints in the proposed method results in better extraction performance. However, PFP was originally developed for EMG decomposition. Unlike ECG signals, EMG signals lack regularity and periodicity. Therefore, in this study, considering the physiological characteristics of extracting FECG and MECG signals, we applied a periodic constrained FastICA algorithm, further adapting it for extracting periodic ECG signals. It can be seen that even in signals with lower noise levels, the performance of morphology-based methods and basic FastICA is significantly affected, but our proposed method still maintains good performance. We also observe that although CycleGAN, a deep learning method, outperforms traditional LMS and FastICA, deep learning methods are data-driven and thus are susceptible to the quality of training data. Additionally, they require large amounts of data and consume considerable computational resources. Moreover, this method uses

Table 6 Comparative evaluation for the FECG detection performance of different methods on public dataset

Method	Year	Channel	Database	Recordings	SEN (%)	PPV (%)	ACC (%)	F1 (%)
TS+PCA[1]	2014	1	NIFECGA	14	94.7	96	-	95.4
			Private data		89.9	88.8	-	89.3
Extended Kalman Smoother[2]	2014	3	NIFECGA	69	97.4	97.2	96	97.3
			private data	24	85.8	85	82.8	85.4
FastICA+SVD[4]	2014	4	NIFECGA	69	99.1	98.9	-	98.99
ANC+SVD[6]	2017	1	ADFECG	2	99.37	99.49	98.90	99.45
			Private data		98.31	98.86	97.21	98.58
NMF[8]	2020	1	ADFECG	5	95.3	94.6	-	94.8
nonlinear estimation[13]	2019	1	ADFECG	5	93.8	98.48	92.41	96.04
			NIFECGA	15	98.63	99.52	97.77	98.85
ST+Shannon Energy	2022	1	ADFECG	4	96.6	96.6	100	98.27
			NIFECGA	20	97.37	98.61	98.72	98.67
CycleGAN[5]	2021	1	ADFECG	5	99.4	99.6	-	99.7
			NIFECGA	68	96.8	97.2	-	97.9
DP-LSTM network[14]	2022	1	ADFECG	22	97.3	98.09	95.53	97.7
			NIFECGA	69	94.2	96.5	91.34	95.3
PA ² Net[15]	2022	1	ADFECG	5	99.58	99.67	-	99.62
			NIFECGA	68	98.9	98.83	-	98.86
CA-KICA[17]	2023	4	ADFECG	5	98.4	97.6	-	98.0
			NIFECGA	69	99.3	99.6	-	99.5
Proposed Method	2024	4	ADFECG	5	99.42%	99.68%	99.74%	99.71%
			NIFECGA	68	99.46%	99.26%	98.75%	99.36%

single-channel signals, so when information in the channels is submerged by significant noise and artifacts, the algorithm cannot process it. In contrast, our proposed method, based on blind source separation principles, integrates spatiotemporal information from multiple channels, resulting in better extraction performance under significant noise without the need for pre-training.

For clinical data shown in Figure 11, we can also observe that Figure 11(a) represents two out of sixteen channels, where the FECG in these channels is not prominent, and there is significant baseline fluctuation. Consequently, even after removing MECG, the signals initially separated by FastICA still cannot accurately identify FECG. However, by utilizing the proposed method to refine the initially extracted signals with periodic constrained FastICA, the extracted FECG becomes more accurate, achieving excellent extraction results as shown in Table 5. Other methods, due to the mentioned drawbacks in the above discussion, therefore, did not achieve results as effective as the proposed method.

It is worth mentioning that in the ablative experiments section as shown in Figure 9, we not only demonstrated the effectiveness of the periodic constrained FastICA module (which has been extensively discussed earlier), but also validated the effectiveness of SVD. It can be seen that replacing least squares in tradition PFP with SVD improve the algorithm's performance. This is because it is difficult to satisfy the assumption in the original data model that the sum of noises is white Gaussian noise with zero mean, as the AECG is interfered by various unpredictable noises like EMG noise and fetal movement. When directly estimating the waveform using the ECG spike train, the noise around the spike may be considered as the desired waveform, leading to inaccurate extraction. When using SVD, we applied a trapezoidal window (whose length depended on the mean RR-interval on the whole record) to select and weight the signal around each detected maternal QRS. This operation allows us to avoid artifacts due to abrupt signal truncation[4]. Therefore, the extracted signal has a better degree of restoration, leading to a better FECG extraction performance.

Regarding the algorithm's peel-off strategy, its effect in avoiding local convergence of the algorithm is challenging to quantitatively describe. However, in experiments, for the preprocessed signals, when we initially execute FastICA for preliminary separation, the separated source signals often do not contain weak FECG sources (although sometimes FECG is extracted in the first round of peel-off). As shown in Figure 11, in the preprocessed original signals (a), the amplitudes of MECG and noise are much larger than FECG. Therefore, after the first round of separation, we obtain the MECG signal and its spikes. When we estimate waveforms using SVD and execute the peel-off step to subtract them from the initial signals, we obtain the residual signals shown in (c). When performing the next round of FastICA and subsequent steps on the residual signals, we find that FECG signals not discovered in the first round can be extracted. This is because removing larger components improves the problem of local convergence of the algorithm. This is also a common technique used in blind source separation. [50, 52] also explains the mechanism of peel-off and emphasizes its significant role in enabling the algorithm to identify weak signals.

Currently, the limitation of our study is that it's an offline algorithm, hence unable to monitor fetal heart in real-time. However, inspired by Zhao et al.'s recent development of an online algorithm for EMG decomposition[64-66], in the future, we can design an online FECG extraction algorithm for real-time fetal heart monitoring.

VI. CONCLUSION

This research reported a FastICA based peel-off framework for ECG extraction from the AECG signal. By incorporating the pcfICA and peel-off strategy, the proposed framework show efficiency in FECG extraction from the AECG. The framework was validated on public datasets, synthetic data and clinical data. It is indicated that our method is a promising technique for maternal and fetal ECG monitoring application.

REFERENCES

- [1] J. Behar, A. Johnson, G. D. Clifford, and J. Oster, "A comparison of single channel fetal ecg extraction methods," *Annals of Biomedical Engineering*, vol. 42, no. 6, pp. 1340-1353, 2014.
- [2] F. Andreotti, M. Riedl, T. Himmelsbach, D. Wedekind, N. Wessel, H. Stepan, C. Schmieder, A. Jank, H. Malberg, and S. Zauneder, "Robust fetal ECG extraction and detection from abdominal leads," *Physiological Measurement*, vol. 35, no. 8, pp. 1551-1567, 2014.
- [3] J. Behar, A. Johnson, G. Clifford, and J. Oster, "A Comparison of Single Channel Fetal ECG Extraction Methods," *Annals of biomedical engineering*, vol. 42, 03/07, 2014.
- [4] M. Varanini, G. Tartarisco, L. Billeci, A. Macerata, G. Pioggia, and R. Balocchi, "An efficient unsupervised fetal QRS complex detection from abdominal maternal ECG," *Physiological Measurement*, vol. 35, no. 8, pp. 1607-1619, Aug, 2014.
- [5] M. R. Mohebbian, S. S. Vedaiei, K. A. Wahid, A. Dinh, H. R. Marateb, and K. Tavakolian, "Fetal ECG Extraction From Maternal ECG Using Attention-Based CycleGAN," *IEEE Journal of Biomedical and Health Informatics*, vol. 26, no. 2, pp. 515-526, 2022.
- [6] N. Zhang, J. Zhang, H. Li, O. O. Mumini, O. W. Samuel, K. Ivanov, and L. Wang, "A novel technique for fetal ECG extraction using single-channel abdominal recording," *Sensors*, vol. 17, no. 3, pp. 457, 2017.
- [7] C. Krüger, "Stillbirths and neonatal deaths: a neglected global pandemic," *Archives of Disease in Childhood*, vol. 108, no. 11, pp. 895-896, Nov, 2023.
- [8] D. Gurve, and S. Krishnan, "Separation of Fetal-ECG From Single-Channel Abdominal ECG Using Activation Scaled Non-Negative Matrix Factorization," *IEEE J Biomed Health Inform*, vol. 24, no. 3, pp. 669-680, Mar, 2020.
- [9] S.-Y. Tsui, C.-S. Liu, and C.-W. Lin, "Modified maternal ECG cancellation for portable fetal heart rate monitor," *Biomedical Signal Processing and Control*, vol. 32, pp. 76-81, 2017/02/01/, 2017.
- [10] F. Marzbanrad, Y. Kimura, K. Funamoto, S. Oshio, M. Endo, N. Sato, M. Palaniswami, and A. H. Khandoker, "Model-based estimation of aortic and mitral valves opening and closing timings in developing human fetuses," *IEEE Journal of Biomedical and Health Informatics*, vol. 20, no. 1, pp. 240-248, 2016.
- [11] T. Li, "Fetal Electrocardiography Extraction Based on Improved Fast Independent Components Analysis Algorithm," *Critical Reviews in Biomedical Engineering*, vol. 49, no. 4, pp. 53-64, 2021.
- [12] P. Olofsson, "Current status of intrapartum fetal monitoring: Cardiotocography versus cardiotocography + ST analysis of the fetal ECG." pp. S113-S118.
- [13] R. G. John, and K. Ramachandran, "Extraction of foetal ECG from abdominal ECG by nonlinear transformation and estimations," *Computer Methods and Programs in Biomedicine*, vol. 175, pp. 193-204, 2019.
- [14] A. Shokouhmand, and N. Tavassolian, "Fetal electrocardiogram extraction using dual-path source separation of single-channel

- non-invasive abdominal recordings,” *IEEE Transactions on Biomedical Engineering*, vol. 70, no. 1, pp. 283-295, 2022.
- [15] X. Wang, Z. He, Z. Lin, Y. Han, T. Liu, J. Lu, and S. Xie, “PA2Net: Period-Aware Attention Network for Robust Fetal ECG Detection,” *IEEE Transactions on Instrumentation and Measurement*, vol. 71, 2022.
- [16] X. Wang, Z. He, Z. Lin, Y. Han, W. Su, and S. Xie, “Correlation-Aware Attention CycleGAN for Accurate Fetal ECG Extraction,” *IEEE Transactions on Instrumentation and Measurement*, pp. 1-1, 2023.
- [17] L. Qiao, S. Hu, B. Xiao, X. Bi, W. Li, and X. Gao, “A Dual Self-Calibrating Framework for Noninvasive Fetal ECG R-Peak Detection,” *IEEE Internet of Things Journal*, vol. 10, no. 18, pp. 16579-16593, 2023.
- [18] A. Wacker-Gussmann, J. F. Strasburger, and R. T. Wakai, “Contribution of Fetal Magnetocardiography to Diagnosis, Risk Assessment, and Treatment of Fetal Arrhythmia,” *Journal of the American Heart Association*, vol. 11, no. 15, Aug 2, 2022.
- [19] X. Wang, Y. Han, and Y. Deng, “CSGSA-Net: Canonical-structured graph sparse attention network for fetal ECG estimation,” *Biomedical Signal Processing and Control*, vol. 82, 2023.
- [20] M. A. Hasan, M. B. I. Reaz, M. I. Ibrahimy, M. S. Hussain, and J. Uddin, “Detection and processing techniques of FECG signal for fetal monitoring,” *Biological Procedures Online*, vol. 11, no. 1, pp. 263-295, 2009.
- [21] X. Wang, Y. Han, and Y. Deng, “ASW-Net: Adaptive Spectral Wavelet Network for Accurate Fetal ECG Extraction,” *IEEE Transactions on Biomedical Circuits and Systems*, vol. 16, no. 6, pp. 1387-1396, 2022.
- [22] A. J. D. Krupa, S. Dhanalakshmi, and R. Kumar, “Joint time-frequency analysis and non-linear estimation for fetal ECG extraction,” *Biomedical Signal Processing and Control*, vol. 75, pp. 103569, 2022.
- [23] A. M. S. S. Kumar, E. E. Nithila, and B. M., “Detection of Fetal Cardiac Anomaly from Composite Abdominal Electrocardiogram,” *Biomedical Signal Processing and Control*, vol. 65, 2021.
- [24] R. Martinek, K. Barnova, R. Jaros, R. Kahankova, T. Kupka, M. Jezewski, R. Czabanski, A. Matonia, J. Jezewski, and K. Horoba, “Passive Fetal Monitoring by Advanced Signal Processing Methods in Fetal Phonocardiography,” *Ieee Access*, vol. 8, pp. 221942-221962, 2020.
- [25] R. Kahankova, M. Mikolasova, R. Jaros, K. Barnova, M. Ladrova, and R. Martinek, “A Review of Recent Advances and Future Developments in Fetal Phonocardiography,” *Ieee Reviews in Biomedical Engineering*, vol. 16, pp. 653-671, 2023.
- [26] D. Edwin Dhas, and M. Suchetha, “Extraction of Fetal ECG from Abdominal and Thorax ECG Using a Non-Causal Adaptive Filter Architecture,” *IEEE Transactions on Biomedical Circuits and Systems*, vol. 16, no. 5, pp. 981-990, 2022.
- [27] S. R. Breesha, and S. S. Vinsley, “Automated Extraction of Fetal ECG Signal Features Using Twinned Filter and Integrated Methodologies,” *Circuits, Systems, and Signal Processing*, 2023.
- [28] M. B. Hossain, S. K. Bashar, J. Lazaro, N. Reljin, Y. Noh, and K. H. Chon, “A robust ECG denoising technique using variable frequency complex demodulation,” *Computer Methods and Programs in Biomedicine*, vol. 200, Mar, 2021.
- [29] W. Zhong, and W. Zhao, “Fetal ECG extraction using short time Fourier transform and generative adversarial networks,” *Physiological Measurement*, vol. 42, no. 10, 2021.
- [30] A. Jaba Deva Krupa, S. Dhanalakshmi, and R. Kumar, “Joint time-frequency analysis and non-linear estimation for fetal ECG extraction,” *Biomedical Signal Processing and Control*, vol. 75, 2022.
- [31] G. J. J. Warmerdam, R. Vullings, L. Schmitt, J. O. E. H. Van Laar, and J. W. M. Bergmans, “Hierarchical probabilistic framework for fetal R-peak detection, using ECG waveform and heart rate information,” *IEEE Transactions on Signal Processing*, vol. 66, no. 16, pp. 4388-4397, 2018.
- [32] A. Jiménez-González, and N. Castañeda-Villa, “Blind extraction of fetal and maternal components from the abdominal electrocardiogram: An ICA implementation for low-dimensional recordings,” *Biomedical Signal Processing and Control*, vol. 58, 2020.
- [33] L. Wang, C. Zhao, M. Dong, and K. Ota, “Fetal ECG Signal Extraction From Long-Term Abdominal Recordings Based on Adaptive QRS Removal and Joint Blind Source Separation,” *IEEE Sensors Journal*, vol. 22, no. 21, pp. 20718-20729, 2022.
- [34] R. Martinek, and J. Židek, “A system for improving the diagnostic quality of fetal electrocardiogram,” *Przeglad Elektrotechniczny*, vol. 88, no. 5 B, pp. 164-173, 2012.
- [35] S. Wu, Y. Shen, Z. Zhou, L. Lin, Y. Zeng, and X. Gao, “Research of fetal ECG extraction using wavelet analysis and adaptive filtering,” *Computers in Biology and Medicine*, vol. 43, no. 10, pp. 1622-1627, 2013.
- [36] R. Jaros, R. Martinek, and R. Kahankova, “Non-Adaptive Methods for Fetal ECG Signal Processing: A Review and Appraisal,” *Sensors*, vol. 18, no. 11, Nov, 2018.
- [37] S. M. M. Martens, C. Rabotti, M. Mischi, and R. J. Sluijter, “A robust fetal ECG detection method for abdominal recordings,” *Physiological Measurement*, vol. 28, no. 4, pp. 373-388, 2007.
- [38] P. P. Kanjilal, S. Palit, and G. Saha, “Fetal ECG extraction from single-channel maternal ECG using singular value decomposition,” *IEEE Transactions on Biomedical Engineering*, vol. 44, no. 1, pp. 51-59, 1997.
- [39] O. G. Viunytskyi, V. I. Shulgin, A. A. Roienko, A. V. Totsky, and K. O. Eguiazarian, “FETAL ECG EXTRACTION FROM THE ABDOMINAL SIGNAL USING WAVELET BISPECTRUM TECHNIQUE,” *Telecommunications and Radio Engineering (English translation of Elektrosyvyaz and Radiotekhnika)*, vol. 82, no. 9, pp. 29-46, 2023.
- [40] P. Darsana, and V. N. Kumar, “Extracting Fetal ECG Signals Through a Hybrid Technique Utilizing Two Wavelet-Based Denoising Algorithms,” *IEEE Access*, vol. 11, pp. 91696-91708, 2023.
- [41] Y. Zhang, A. Gu, Z. Xiao, Z. Cai, C. Yang, J. Li, and C. Liu, “Fetal Heart Rate Extraction from Abdominal Electrocardiography Recordings Based on Wavelet Transform and Adaptive Threshold Algorithm.”
- [42] H. Ghonchi, and V. Abolghasemi, “A Dual Attention-Based Autoencoder Model for Fetal ECG Extraction From Abdominal Signals,” *IEEE Sensors Journal*, vol. 22, no. 23, pp. 22908-22918, 2022.
- [43] Z. Zhou, K. Huang, Y. Qiu, H. Shen, and Z. Ming, “Morphology extraction of fetal electrocardiogram by slow-fast LSTM network,” *Biomedical Signal Processing and Control*, vol. 68, 2021.
- [44] A. Mohammed Kaleem, and R. D. Kokate, “A survey on FECG extraction using neural network and adaptive filter,” *Soft Computing*, vol. 25, no. 6, pp. 4379-4392, 2021.
- [45] M. Varanini, G. Tartarisco, R. Balocchi, A. Macerata, G. Pioggia, and L. Billeci, “A new method for QRS complex detection in multichannel ECG: Application to self-monitoring of fetal health,” *Computers in Biology and Medicine*, vol. 85, pp. 125-134, 2017.
- [46] R. Sameni, C. Jutten, and M. B. Shamsollahi, “Multichannel electrocardiogram decomposition using periodic component analysis,” *IEEE Transactions on Biomedical Engineering*, vol. 55, no. 8, pp. 1935-1940, 2008.
- [47] H. W. Zhao, X. Zhang, M. Q. Chen, and P. Zhou, “Online Decomposition of Surface Electromyogram Into Individual Motor Unit Activities Using Progressive FastICA Peel-Off,” *Ieee Transactions on Biomedical Engineering*, vol. 71, no. 1, pp. 160-170, Jan, 2024.
- [48] M. Q. Chen, X. Zhang, and P. Zhou, “Automatic Multichannel Intramuscular Electromyogram Decomposition: Progressive FastICA Peel-Off and Performance Validation,” *Ieee Transactions on Neural Systems and Rehabilitation Engineering*, vol. 27, no. 1, pp. 76-84, Jan, 2019.
- [49] M. Q. Chen, X. Zhang, Z. Y. Lu, X. Y. Li, and P. Zhou, “Two-Source Validation of Progressive FastICA Peel-Off for Automatic Surface EMG Decomposition in Human First Dorsal Interosseous Muscle,” *International Journal of Neural Systems*, vol. 28, no. 9, Nov, 2018.
- [50] M. Q. Chen, X. Zhang, X. Chen, and P. Zhou, “Automatic Implementation of Progressive FastICA Peel-Off for High Density Surface EMG Decomposition,” *Ieee Transactions on Neural Systems and Rehabilitation Engineering*, vol. 26, no. 1, pp. 144-152, Jan, 2018.
- [51] M. Q. Chen, A. Holobar, X. Zhang, and P. Zhou, “Progressive FastICA Peel-Off and Convolution Kernel Compensation

- Demonstrate High Agreement for High Density Surface EMG Decomposition,” *Neural Plasticity*, vol. 2016, 2016.
- [52] M. Q. Chen, and P. Zhou, “A Novel Framework Based on FastICA for High Density Surface EMG Decomposition,” *Ieee Transactions on Neural Systems and Rehabilitation Engineering*, vol. 24, no. 1, pp. 117-127, Jan, 2016.
- [53] C. L. Zhang, X. G. Zhang, M. Q. Zhang, and Y. D. Li, “Neighbor number, valley seeking and clustering,” *Pattern Recognition Letters*, vol. 28, no. 2, pp. 173-180, Jan 15, 2007.
- [54] M. Q. Chen, X. Zhang, X. Chen, M. X. Zhu, G. L. Li, and P. Zhou, “FastICA peel-off for ECG interference removal from surface EMG,” *Biomedical Engineering Online*, vol. 15, Jun 13, 2016.
- [55] F. Negro, S. Muceli, A. M. Castronovo, A. Holobar, and D. Farina, “Multi-channel intramuscular and surface EMG decomposition by convolutive blind source separation,” *Journal of Neural Engineering*, vol. 13, no. 2, Apr, 2016.
- [56] A. L. Goldberger, L. A. N. Amaral, L. Glass, J. M. Hausdorff, P. C. Ivanov, R. G. Mark, J. E. Mietus, G. B. Moody, C. K. Peng, and H. E. Stanley, “PhysioBank, PhysioToolkit, and PhysioNet - Components of a new research resource for complex physiologic signals,” *Circulation*, vol. 101, no. 23, pp. E215-E220, Jun 13, 2000.
- [57] I. Silva, J. Behar, R. Sameni, T. T. Zhu, J. Oster, G. D. Clifford, and G. B. Moody, “Noninvasive Fetal ECG: the PhysioNet/Computing in Cardiology Challenge 2013,” *2013 Computing in Cardiology Conference (Cinc)*, vol. 40, pp. 149-152, 2013.
- [58] M. Varanini, G. Tartarisco, L. Billeci, A. Macerata, G. Pioggia, and R. Balocchi, “A multi-step approach for non-invasive fetal ECG analysis.” pp. 281-284.
- [59] F. Andreotti, J. Behar, S. Zaunseder, J. Oster, and G. D. Clifford, “An open-source framework for stress-testing non-invasive foetal ECG extraction algorithms,” *Physiological Measurement*, vol. 37, no. 5, pp. 627, 2016/04/12, 2016.
- [60] J. Behar, F. Andreotti, S. Zaunseder, Q. Li, J. Oster, and G. D. Clifford, “An ECG simulator for generating maternal-foetal activity mixtures on abdominal ECG recordings,” *Physiological Measurement*, vol. 35, no. 8, pp. 1537, 2014/07/28, 2014.
- [61] Z. Wang, “Fixed-point algorithms for constrained ICA and their applications in fMRI data analysis,” *Magnetic resonance imaging*, vol. 29, no. 9, pp. 1288-1303, 2011.
- [62] R. Macwan, Y. Benezeth, and A. Mansouri, “Remote photoplethysmography with constrained ICA using periodicity and chrominance constraints,” *Biomedical engineering online*, vol. 17, no. 1, pp. 1-22, 2018.
- [63] W. Zhong, L. Liao, X. Guo, and G. Wang, “A deep learning approach for fetal QRS complex detection,” *Physiological Measurement*, vol. 39, no. 4, 2018.
- [64] H. Zhao, Y. Sun, C. Wei, Y. Xia, P. Zhou, and X. Zhang, “Online prediction of sustained muscle force from individual motor unit activities using adaptive surface EMG decomposition,” *J Neuroeng Rehabil*, vol. 21, no. 1, pp. 47, Apr 4, 2024.
- [65] H. Zhao, X. Zhang, M. Chen, and P. Zhou, “Adaptive Online Decomposition of Surface EMG Using Progressive FastICA Peel-Off,” *IEEE Trans Biomed Eng*, vol. 71, no. 4, pp. 1257-1268, Apr, 2024.
- [66] H. Zhao, X. Zhang, M. Chen, and P. Zhou, “Online Decomposition of Surface Electromyogram Into Individual Motor Unit Activities Using Progressive FastICA Peel-Off,” *IEEE Trans Biomed Eng*, vol. 71, no. 1, pp. 160-170, Jan, 2024.